

# Fundamentals of Power Semiconductor Devices

B. Jayant Baliga

# Fundamentals of Power Semiconductor Devices

 Springer

B. Jayant Baliga  
Power Semiconductor Research Center  
North Carolina State University  
1010 Main Campus Drive  
Raleigh, NC 27695-7924  
USA

ISBN 978-0-387-47313-0

e-ISBN 978-0-387-47314-7

Library of Congress Control Number: 2008923040

© 2008 Springer Science + Business Media, LLC

All rights reserved. This work may not be translated or copied in whole or in part without the written permission of the publisher (Springer Science+Business Media, LLC, 233 Spring Street, New York, NY 10013, USA), except for brief excerpts in connection with reviews or scholarly analysis. Use in connection with any form of information storage and retrieval, electronic adaptation, computer software, or by similar or dissimilar methodology now known or hereafter developed is forbidden.

The use in this publication of trade names, trademarks, service marks and similar terms, even if they are not identified as such, is not to be taken as an expression of opinion as to whether or not they are subject to proprietary rights.

Printed on acid-free paper.

9 8 7 6 5 4 3 2 1

springer.com

## **Dedication**

*The author would like to dedicate this book to his wife, Pratima, for her unwavering support throughout his career devoted to the enhancement of the performance and understanding of power semiconductor devices.*

# Preface

Today the semiconductor business exceeds \$200 billion with about 10% of the revenue derived from power semiconductor devices and smart power integrated circuits. Power semiconductor devices are recognized as a key component for all power electronic systems. It is estimated that at least 50% of the electricity used in the world is controlled by power devices. With the widespread use of electronics in the consumer, industrial, medical, and transportation sectors, power devices have a major impact on the economy because they determine the cost and efficiency of systems. After the initial replacement of vacuum tubes by solid-state devices in the 1950s, semiconductor power devices have taken a dominant role with silicon serving as the base material. These developments have been referred to as the *Second Electronic Revolution*.

Bipolar power devices, such as bipolar transistors and thyristors, were first developed in the 1950s. Because of the many advantages of semiconductor devices compared with vacuum tubes, there was a constant demand for increasing the power ratings of these devices. Their power rating and switching frequency increased with advancements in the understanding of the operating physics, the availability of larger diameter, high resistivity silicon wafers, and the introduction of more advanced lithography capability. During the next 20 years, the technology for the bipolar devices reached a high degree of maturity. By the 1970s, bipolar power transistors with current handling capability of hundreds of amperes and voltage blocking capability of over 500 V became available. More remarkably, technology was developed capable of manufacturing an individual power thyristor from an entire 4-inch diameter silicon wafer with voltage rating over 5,000 V.

My involvement with power semiconductor devices began in 1974 when I was hired by the General Electric Company at their corporate research and development center to start a new group to work on this technology. At that time, I had just completed my Ph.D. degree at Rensselaer Polytechnic Institute by

performing research on a novel method for the growth of epitaxial layers of compound semiconductors.<sup>1-4</sup> Although I wanted to explore this approach after joining the semiconductor industry, I was unable to secure a position at any of the major research laboratories due to a lack of interest in this unproven growth technology. Ironically, the OMCVD epitaxial growth process that I pioneered with Professor Ghandhi has now become the most commonly used method for the growth of high quality compound semiconductor layers for applications such as lasers, LEDs, and microwave transistors.

My first assignment at GE was to develop improved processes for the fabrication of high voltage thyristors used in their power distribution business. Since the thyristors were used for high voltage DC transmission and electric locomotive drives, the emphasis was on increasing the voltage rating and current handling capability. The ability to use neutron transmutation doping to produce high resistivity n-type silicon with improved uniformity across large diameter wafers became of interest at this time. I was fortunate in making some of the critical contributions to annealing the damage caused to the silicon lattice during neutron irradiation making this process commercially viable.<sup>5</sup> This enabled increasing the blocking voltage of thyristors to over 5,000 V while being able to handle over 2,000 A of current in a single device.

Meanwhile, bipolar power transistors were being developed with the goal of increasing the switching frequency in medium power systems. Unfortunately, the current gain of bipolar transistors was found to be low when it was designed for high voltage operation at high current density. The popular solution to this problem, using the Darlington configuration, had the disadvantage of increasing the on-state voltage drop resulting in an increase in the power dissipation. In addition to the large control currents required for bipolar transistors, they suffered from poor safe-operating-area due to second breakdown failure modes. These issues produced a cumbersome design, with snubber networks, that raised the cost and degraded the efficiency of the power control system.

In the 1970s, the power MOSFET product was first introduced by International Rectifier Corporation. Although initially hailed as a replacement for all bipolar power devices due to its high input impedance and fast switching speed, the power MOSFET has successfully cornered the market for low voltage (<100 V) and high switching speed (>100 kHz) applications but failed to make serious inroads in the high voltage arena. This is because the on-state resistance of power MOSFETs increases very rapidly with increase in the breakdown voltage. The resulting high conduction losses, even when using larger more expensive die, degrade the overall system efficiency.

In recognition of these issues, I proposed two new thrusts in 1979 for the power device field. The first was based upon the merging of MOS and bipolar device physics to create a new category of power devices.<sup>6</sup> My most successful innovation among MOS-bipolar devices has been the insulated gate bipolar transistor (IGBT). Soon after commercial introduction in the early 1980s, the IGBT was adopted for all medium power electronic applications. Today, it is

manufactured by more than a dozen companies around the world for consumer, industrial, medical, and other applications that benefit society. The triumph of the IGBT is associated with its huge power gain, high input impedance, wide safe operating area, and a switching speed that can be tailored for applications depending upon their operating frequency.

The second approach that I suggested in 1979 for enhancing the performance of power devices was to replace silicon with wide bandgap semiconductors. The basis for this approach was an equation that I derived relating the on-resistance of the drift region in unipolar power devices to the basic properties of the semiconductor material. This equation has since been referred to as Baliga's figure of merit (BFOM). In addition to the expected reduction in the on-state resistance with higher carrier mobility, the equation predicts a reduction in on-resistance as the inverse of the cube of the breakdown electric field strength of the semiconductor material.

The first attempt to develop wide-bandgap-semiconductor-based power devices was undertaken at the General Electric Corporate Research and Development Center, Schenectady, NY, under my direction. The goal was to leverage a 13-fold reduction in specific on-resistance for the drift region predicted by the BFOM for gallium arsenide. A team of ten scientists was assembled to tackle the difficult problems of the growth of high resistivity epitaxial layers, the fabrication of low resistivity ohmic contacts, low leakage Schottky contacts, and the passivation of the GaAs surface. This led to an enhanced understanding of the breakdown strength<sup>7</sup> for GaAs and the successful fabrication of high performance Schottky rectifiers<sup>8</sup> and MESFETs.<sup>9</sup> Experimental verification of the basic thesis of the analysis represented by BFOM was therefore demonstrated during this period. Commercial GaAs-based Schottky rectifier products were subsequently introduced in the market by several companies.

In the later half of the 1980s, the technology for the growth of silicon carbide was developed at North Carolina State University (NCSU) with the culmination of commercial availability of wafers from CREE Research Corporation. Although data on the impact ionization coefficients of SiC were not available, early reports on the breakdown voltage of diodes enabled estimation of the breakdown electric field strength. Using these numbers in the BFOM predicted an impressive 100–200-fold reduction in the specific on-resistance of the drift region for SiC-based unipolar devices. In 1988, I joined NCSU and subsequently founded the Power Semiconductor Research Center (PSRC) – an industrial consortium – with the objective of exploring ideas to enhance power device performance. Within the first year of the inception of the program, SiC Schottky barrier rectifiers with breakdown voltage of 400 V were successfully fabricated with on-state voltage drop of about 1 V and no reverse recovery transients.<sup>10</sup> By improving the edge termination of these diodes, the breakdown voltage was found to increase to 1,000 V. With the availability of epitaxial SiC material with lower doping concentrations, SiC Schottky rectifiers with breakdown voltages over 2.5 kV have been fabricated at PSRC.<sup>11</sup> These results have motivated many other

groups around the world to develop SiC-based power rectifiers. In this regard, it has been my privilege to assist in the establishment of national programs to fund research on silicon carbide technology in the United States, Japan, and Switzerland–Sweden. Meanwhile, accurate measurements of the impact ionization coefficients for 6H-SiC and 4H-SiC in defect-free regions were performed at PSRC using an electron beam excitation method.<sup>12</sup> Using these coefficients, a BFOM of over 1,000 is predicted for SiC, providing even greater motivation to develop power devices from this material.

Although the fabrication of high performance, high voltage Schottky rectifiers has been relatively straightforward, the development of a suitable silicon carbide MOSFET structure has been problematic. The existing silicon power D-MOSFET and U-MOSFET structures do not directly translate to suitable structures in silicon carbide. The interface between SiC and silicon dioxide, as a gate dielectric, needed extensive investigation due to the large density of traps that prevent the formation of high conductivity inversion layers. Even after overcoming this hurdle, the much higher electric field in the silicon dioxide when compared with silicon devices, resulting from the much larger electric field in the underlying SiC, leads to reliability problems. Fortunately, a structural innovation called the ACCUFET, to overcome both of these problems, was proposed and demonstrated at PSRC.<sup>13</sup> In this structure, a buried P<sup>+</sup> region is used to shield the gate region from the high electric field within the SiC drift region. This concept is applicable to devices that utilize either accumulation channels or inversion channels. Devices with low specific on-resistance have been demonstrated at PSRC using both 6H-SiC and 4H-SiC with epitaxial material capable of supporting over 5,000 V.<sup>14</sup> This device structure has been subsequently emulated by several groups around the world.

The availability of power semiconductor devices with high input impedance has encouraged the development of integrated control circuits. In general, the integration of the control circuit is preferred over the discrete counterpart due to reduced manufacturing costs at high volumes and improved reliability from a reduction of the interconnects. Since the complexity of including additional circuitry to an IC is relatively small, the incorporation of protective features such as over-temperature, over-current, and over-voltage has become cost effective. In addition, the chips can contain encode/decode CMOS circuitry to interface with a central microprocessor or computer in the system for control and diagnostic purposes. This technology is commonly referred to as *Smart Power Technology*.<sup>15</sup>

The advent of smart power technology portends a *Second Electronic Revolution*. In contrast to the integrated circuits for information processing, this technology enables efficient control of power and energy. These technologies can therefore be regarded as complementary, similar to the brain and muscles in the human body. Smart power technology is having an enormous impact on society. The widespread use of power semiconductor devices in consumer, industrial, transportation, and medical applications brings greater mobility and comfort to

billions of people around the world. Our ability to improve the efficiency for the control of electric power results in the conservation of fossil fuels, which in turn provides reduction of environmental pollution.

Due to these developments, it is anticipated that there will be an increasing need for technologists trained in the discipline of designing and manufacturing power semiconductor devices. This textbook provides the knowledge in a tutorial format suitable for self-study or in a graduate/senior level university course. In comparison with my previous textbooks<sup>16,17</sup> (which have gone out of print), this book provides a more detailed description of the operating physics of power devices. Analytical expressions have been rigorously derived using the fundamental semiconductor Poisson's, continuity, and conduction equations. The electrical characteristics of all the power devices discussed in this book can be computed using these analytical solutions as shown by typical examples provided in each section. Due to increasing interest in the utilization of wide bandgap semiconductors for power devices, the book includes the analysis of silicon carbide structures. To corroborate the validity of the analytical formulations, I have included the results of two-dimensional numerical simulations using MEDICI<sup>18</sup> in each section of the book. The simulation results are also used to elucidate further the physics and point out two-dimensional effects whenever relevant.

In Chap. 1, a broad introduction to potential applications for power devices is provided. The electrical characteristics for ideal power rectifiers and transistors are then defined and compared with those for typical devices. Chapter 2 provides the transport properties of silicon and silicon carbide that have relevance to the analysis and performance of power device structures. Chapter 3 discusses breakdown voltage, which is the most unique distinguishing characteristic for power devices, together with edge termination structures. This analysis is pertinent to all the device structures discussed in subsequent chapters of the book.

Chapter 4 provides a detailed analysis of the Schottky rectifier structure. On-state current flow via thermionic emission is described followed by the impact of image force barrier lowering on the reverse leakage current. These phenomena influence the selection of the barrier height to optimize the power losses as described in the chapter. The influence of the tunneling current component is also included in this chapter due to its importance for silicon carbide Schottky rectifiers.

Chapter 5 describes the physics of operation of high voltage P-i-N rectifiers. The theory for both low-level and high-level injection conditions during on-state current flow is developed in detail. The impact of this on the reverse recovery phenomenon during turn-off is then analyzed. The influence of end region recombination, carrier-carrier scattering, and auger recombination are included in the analysis.

In Chap. 6, an extensive discussion of the operating principles and design considerations is provided for the power metal-oxide-semiconductor field effect transistor (MOSFET) structure. The influence of the parasitic bipolar transistor on the blocking voltage is described together with methods for its suppression. The

basic physics of creating channels in the MOSFET structure is then developed. The concepts of threshold voltage, transconductance, and specific on-resistance are described. Various components of the on-state resistance are analyzed and optimization procedures are provided. Both the commercially available DMOS and UMOS structures are analyzed here. The modification of the physics required to produce a superlinear transfer characteristic is included due to its relevance for RF and audio applications. A detailed analysis of the device capacitances is then provided for use in the analysis of the switching behavior. Analysis of the gate charge is included here because of its common use in comparing device designs. The switching characteristics of the power MOSFET are then related to its capacitance, including the impact of the Miller effect. This is followed by discussion of the safe-operating-area, the integral body diode, high temperature characteristics, and complementary (p-channel) devices. A brief description of the process flow for the D-MOSFET and U-MOSFET structures is given in the chapter for completeness. The last portion of the chapter focuses on silicon carbide technology with the options of the Baliga–Pair configuration, the shielded planar structure, and the shielded trench-gate structure described in detail.

Chapter 7 is devoted to bipolar power transistors. The basic theory for current transport and gain in an N–P–N transistor is first developed followed by a discussion of issues relevant to power transistors. The various breakdown modes of the bipolar transistors are then explained. The physics governing the current gain of the bipolar transistor is extensively analyzed including high-level injection effects, the current-induced base, and emitter current crowding. The output characteristics for the bipolar transistor are then described with analysis of the saturation region, the quasisaturation mode, and the output resistance. This is followed by analysis of the switching characteristics. The influence of stored charge on the switching behavior of the bipolar transistor is described in detail during both the turn-on and turn-off transients. Issues dealing with second breakdown are then considered followed by ways to improve the current gain by using the Darlington configuration.

The physics of operation of the power thyristor is considered in Chap. 8. The impact of the four layer structure on the forward and reverse blocking capability is first analyzed including the use of cathode shorts. The on-state characteristics for the thyristor are then shown to approach those for a P–i–N rectifier. The gate triggering and holding currents are related to the cathode short design. Under switching characteristics, the turn-on physics is discussed with description of the involute design, the amplifying gate, and light-activated gate structures. The commutated switching behavior is also analyzed together with a discussion of voltage transients. The basic principles of the gate turn-off (GTO) thyristor are then described with analytical models for the storage, voltage-rise and current-fall times. The chapter concludes with the description of triacs, which are commonly used for AC power control.

The insulated gate bipolar transistor (IGBT) is discussed in depth in Chap. 9. The benefits of controlling bipolar current transport in a wide base P–N–P

transistor using a MOS channel are explained. The design of both reverse blocking (symmetric) and unidirectional blocking (asymmetric) structures is considered here. The on-state characteristics of the IGBT are then extensively analyzed including the impact of high-level injection in the wide-base region and the finite injection efficiency of the collector junction. The discussion includes not only the basic symmetric IGBT structure but also the asymmetric structure and the transparent emitter structure. The utilization of lifetime control is compared with changes to the N-buffer-layer and P<sup>+</sup> collector doping concentrations. After developing the current saturation model for the IGBT structure, the output characteristics for the three types of IGBT structure are derived. The impact of the stored charge on the switching behavior of the device is then analyzed for the case of no-load, resistive-load, and inductive-load conditions for each of the three types of structures. The optimization of the power losses in the IGBT structure is then performed, allowing comparison of the three types of structures. The next section of the chapter describes the complementary (p-channel) IGBT structure. This is followed by an extensive discussion of methods for suppression of the parasitic thyristor in the IGBT due to its importance for designing stable devices. The next section on the safe-operating-area includes analysis of the FBSOA, RBSOA, and SCSOA. The trench-gate IGBT structure is then demonstrated to produce lower on-state voltage drop. This is followed by discussion of scaling up the voltage rating for the IGBT and its excellent characteristics for high ambient temperatures. Various methods for improving the switching speed of the IGBT structure and optimizing its cell structure are then discussed. The chapter concludes with the description of the reverse conducting IGBT structure.

The final chapter (Chap. 10) provides the basis for the comparison of various power devices from an applications viewpoint. A typical motor drive case is selected to demonstrate the reduction of power losses by optimization of the on-state and switching characteristics of the devices. The importance of reducing the reverse recovery current in power rectifiers is highlighted here.

Throughout the book, emphasis is placed on deriving simple analytical expressions that describe the underlying physics and enable representation of the device electrical characteristics. This treatment is invaluable for teaching a course on power devices because it allows the operating principles and concepts to be conveyed with quantitative analysis. The analytical approach used in the book based on physical insight will provide a good foundation for the reader. The results of two-dimensional numerical simulations have been included to supplement and reinforce the concepts. Due to space limitations, only the basic power device structures have been included in this book. Advanced structures will be covered in monographs to be subsequently published. I am hopeful that this book will be widely used for the teaching of courses on solid-state devices and that it will become an essential reference for the power device industry well into the future.

## References

---

- <sup>1</sup> B.J. Baliga and S.K. Ghandhi, “Heteroepitaxial InAs Grown on GaAs from Triethylindium and Arsine”, *Journal of the Electrochemical Society*, Vol. 121, pp 1642–1650, 1974.
- <sup>2</sup> B.J. Baliga and S.K. Ghandhi, “Growth and Properties of Heteroepitaxial GaInAs Alloys Grown on GaAs Substrates from Trimethylgallium, Triethylindium and Arsine”, *Journal of the Electrochemical Society*, Vol. 122, pp 683–687, 1975.
- <sup>3</sup> B.J. Baliga and S.K. Ghandhi, “The Preparation and Properties of Tin Oxide Films Formed by the Oxidation of Trimethyltin”, *Journal of the Electrochemical Society*, Vol. 123, pp 941–944, 1976.
- <sup>4</sup> B.J. Baliga and S.K. Ghandhi, “Preparation and Properties of Zinc Oxide Films Grown by the Oxidation of Diethylzinc”, *Journal of the Electrochemical Society*, Vol. 128, pp 558–561, 1981.
- <sup>5</sup> B.J. Baliga et al., “Defect Levels Controlling the Behavior of Neutron Transmutation Doped Silicon during Annealing”, NTD Conference, April 1987.
- <sup>6</sup> B.J. Baliga, “Evolution of MOS-Bipolar Power Semiconductor Technology”, *Proceedings IEEE*, pp 409–418, 1988.
- <sup>7</sup> B.J. Baliga et al., “Breakdown Characteristics of Gallium Arsenide”, *IEEE Electron Device Letters*, Vol. EDL-2, pp 302–304, 1981.
- <sup>8</sup> B.J. Baliga et al., “Gallium Arsenide Schottky Power Rectifiers”, *IEEE Transactions on Electron Devices*, Vol. ED-32, pp 1130–1134, 1985.
- <sup>9</sup> P.M. Campbell et al., “Trapezoidal-Groove Schottky-Gate Vertical-Channel GaAs FET”, *IEEE Electron Device Letters*, Vol. EDL-6, pp 304–306, 1985.
- <sup>10</sup> M. Bhatnagar, P.K. McLarty, and B.J. Baliga, “Silicon-Carbide High-Voltage (400 V) Schottky Barrier Diodes”, *IEEE Electron Device Letters*, Vol. EDL-13, pp 501–503, 1992.
- <sup>11</sup> R.K. Chilukuri and B.J. Baliga, “High Voltage Ni/4H-SiC Schottky Rectifiers”, *IEEE International Symposium on Power Semiconductor Devices and ICs*, pp 161–164, 1999.
- <sup>12</sup> R. Raghunathan and B.J. Baliga, “Temperature dependence of Hole Impact Ionization Coefficients in 4H and 6H-SiC”, *Solid State Electronics*, Vol. 43, pp 199–211, 1999.
- <sup>13</sup> P.M. Shenoy and B.J. Baliga, “High Voltage Planar 6H-SiC ACCUFET”, *International Conference on Silicon Carbide, III-Nitrides, and Related Materials*, Abstract Tu3b-3, pp 158–159, 1997.
- <sup>14</sup> R.K. Chilukuri and B.J. Baliga, PSRC Technical Report TR-00-007, May 2000.
- <sup>15</sup> B.J. Baliga, “Smart Power Technology: An Elephantine Opportunity”, Invited Plenary Talk, *IEEE International Electron Devices Meeting*, pp 3–6, 1990.
- <sup>16</sup> B.J. Baliga, “Modern Power Devices”, Wiley, New York, 1987.
- <sup>17</sup> B.J. Baliga, “Power Semiconductor Devices”, PWS, Boston, MA, 1996.
- <sup>18</sup> MEDICI TCAD Simulator, Avanti Corporation, Fremont, CA 94538.

# Contents

Preface	vii
<b>Chapter 1 Introduction</b>	<b>1</b>
1.1 Ideal and Typical Power Switching Waveforms .....	3
1.2 Ideal and Typical Power Device Characteristics .....	5
1.3 Unipolar Power Devices .....	8
1.4 Bipolar Power Devices.....	10
1.5 MOS-Bipolar Power Devices.....	11
1.6 Ideal Drift Region for Unipolar Power Devices .....	14
1.7 Charge-Coupled Structures: Ideal Specific On-Resistance .....	16
1.8 Summary .....	21
Problems.....	21
References .....	22
<b>Chapter 2 Material Properties and Transport Physics</b>	<b>23</b>
2.1 Fundamental Properties.....	23
2.1.1 Intrinsic Carrier Concentration.....	25
2.1.2 Bandgap Narrowing.....	26
2.1.3 Built-in Potential.....	30
2.1.4 Zero-Bias Depletion Width .....	32
2.1.5 Impact Ionization Coefficients .....	32
2.1.6 Carrier Mobility .....	34
2.2 Resistivity.....	51
2.2.1 Intrinsic Resistivity.....	51
2.2.2 Extrinsic Resistivity.....	51
2.2.3 Neutron Transmutation Doping.....	55
2.3 Recombination Lifetime.....	59

2.3.1	Shockley–Read–Hall Recombination.....	60
2.3.2	Low-Level Lifetime.....	63
2.3.3	Space-Charge Generation Lifetime.....	65
2.3.4	Recombination Level Optimization.....	66
2.3.5	Lifetime Control.....	75
2.3.6	Auger Recombination.....	80
2.4	Ohmic Contacts.....	82
2.5	Summary.....	84
	Problems.....	84
	References.....	86

<b>Chapter 3</b>	<b>Breakdown Voltage.....</b>	<b>91</b>
3.1	Avalanche Breakdown.....	92
3.1.1	Power Law Approximations for the Impact Ionization Coefficients.....	92
3.1.2	Multiplication Coefficient.....	94
3.2	Abrupt One-Dimensional Diode.....	95
3.3	Ideal Specific On-Resistance.....	100
3.4	Abrupt Punch-Through Diode.....	101
3.5	Linearly Graded Junction Diode.....	104
3.6	Edge Terminations.....	107
3.6.1	Planar Junction Termination.....	108
3.6.2	Planar Junction with Floating Field Ring.....	120
3.6.3	Planar Junction with Multiple Floating Field Rings.....	130
3.6.4	Planar Junction with Field Plate.....	132
3.6.5	Planar Junction with Field Plates and Field Rings.....	137
3.6.6	Bevel Edge Terminations.....	137
3.6.7	Etch Terminations.....	148
3.6.8	Junction Termination Extension.....	149
3.7	Open-Base Transistor Breakdown.....	155
3.7.1	Composite Bevel Termination.....	159
3.7.2	Double-Positive Bevel Termination.....	159
3.8	Surface Passivation.....	162
3.9	Summary.....	162
	Problems.....	163
	References.....	164

<b>Chapter 4</b>	<b>Schottky Rectifiers.....</b>	<b>167</b>
4.1	Power Schottky Rectifier Structure.....	168
4.2	Metal–Semiconductor Contact.....	169
4.3	Forward Conduction.....	171
4.4	Reverse Blocking.....	179
4.4.1	Leakage Current.....	180
4.4.2	Schottky Barrier Lowering.....	181
4.4.3	Prebreakdown Avalanche Multiplication.....	184

4.4.4	Silicon Carbide Rectifiers.....	185
4.5	Device Capacitance.....	187
4.6	Thermal Considerations.....	188
4.7	Fundamental Tradeoff Analysis.....	192
4.8	Device Technology.....	194
4.9	Barrier Height Adjustment.....	194
4.10	Edge Terminations.....	197
4.11	Summary.....	198
	Problems.....	199
	References.....	200
<b>Chapter 5</b>	<b>P-i-N Rectifiers.....</b>	<b>203</b>
5.1	One-Dimensional Structure.....	204
5.1.1	Recombination Current.....	205
5.1.2	Low-Level Injection Current.....	206
5.1.3	High-Level Injection Current.....	208
5.1.4	Injection into the End Regions.....	217
5.1.5	Carrier–Carrier Scattering Effect.....	219
5.1.6	Auger Recombination Effect.....	219
5.1.7	Forward Conduction Characteristics.....	221
5.2	Silicon Carbide P-i-N Rectifiers.....	230
5.3	Reverse Blocking.....	232
5.4	Switching Performance.....	236
5.4.1	Forward Recovery.....	236
5.4.2	Reverse Recovery.....	244
5.5	P-i-N Rectifier Structure with Buffer Layer.....	262
5.6	Nonpunch-Through P-i-N Rectifier Structure.....	263
5.7	P-i-N Rectifier Tradeoff Curves.....	270
5.8	Summary.....	274
	Problems.....	275
	References.....	276
<b>Chapter 6</b>	<b>Power MOSFETs.....</b>	<b>279</b>
6.1	Ideal Specific On-Resistance.....	280
6.2	Device Cell Structure and Operation.....	282
6.2.1	The V-MOSFET Structure.....	283
6.2.2	The VD-MOSFET Structure.....	284
6.2.3	The U-MOSFET Structure.....	285
6.3	Basic Device Characteristics.....	286
6.4	Blocking Voltage.....	289
6.4.1	Impact of Edge Termination.....	289
6.4.2	Impact of Graded Doping Profile.....	290
6.4.3	Impact of Parasitic Bipolar Transistor.....	291
6.4.4	Impact of Cell Pitch.....	293

6.4.5	Impact of Gate Shape.....	296
6.4.6	Impact of Cell Surface Topology .....	298
6.5	Forward Conduction Characteristics.....	300
6.5.1	MOS Interface Physics .....	301
6.5.2	MOS Surface Charge Analysis.....	305
6.5.3	Maximum Depletion Width.....	310
6.5.4	Threshold Voltage .....	311
6.5.5	Channel Resistance.....	321
6.6	Power VD-MOSFET On-Resistance .....	327
6.6.1	Source Contact Resistance.....	329
6.6.2	Source Region Resistance .....	330
6.6.3	Channel Resistance.....	331
6.6.4	Accumulation Resistance.....	332
6.6.5	JFET Resistance.....	333
6.6.6	Drift Region Resistance.....	335
6.6.7	N <sup>+</sup> Substrate Resistance.....	339
6.6.8	Drain Contact Resistance.....	339
6.6.9	Total On-Resistance.....	340
6.7	Power VD-MOSFET Cell Optimization.....	343
6.7.1	Optimization of Gate Electrode Width.....	343
6.7.2	Impact of Breakdown Voltage.....	345
6.7.3	Impact of Design Rules .....	348
6.7.4	Impact of Cell Topology.....	350
6.8	Power U-MOSFET On-Resistance .....	358
6.8.1	Source Contact Resistance.....	359
6.8.2	Source Region Resistance .....	361
6.8.3	Channel Resistance.....	361
6.8.4	Accumulation Resistance.....	362
6.8.5	Drift Region Resistance.....	363
6.8.6	N <sup>+</sup> Substrate Resistance.....	364
6.8.7	Drain Contact Resistance.....	365
6.8.8	Total On-Resistance.....	365
6.9	Power U-MOSFET Cell Optimization.....	368
6.9.1	Orthogonal P-Base Contact Structure .....	368
6.9.2	Impact of Breakdown Voltage.....	371
6.9.3	Ruggedness Improvement .....	372
6.10	Square-Law Transfer Characteristics.....	373
6.11	Superlinear Transfer Characteristics .....	377
6.12	Output Characteristics.....	381
6.13	Device Capacitances .....	385
6.13.1	Basic MOS Capacitance .....	386
6.13.2	Power VD-MOSFET Structure Capacitances .....	389
6.13.3	Power U-MOSFET Structure Capacitances .....	399
6.13.4	Equivalent Circuit.....	408

6.14	Gate Charge .....	409
6.14.1	Charge Extraction .....	409
6.14.2	Voltage and Current Dependence .....	417
6.14.3	VD-MOSFET vs. U-MOSFET Structure .....	421
6.14.4	Impact of VD-MOSFET and U-MOSFET Cell Pitch .....	423
6.15	Optimization for High Frequency Operation .....	426
6.15.1	Input Switching Power Loss .....	427
6.15.2	Output Switching Power Loss .....	432
6.15.3	Gate Propagation Delay .....	434
6.16	Switching Characteristics .....	436
6.16.1	Turn-On Transient .....	437
6.16.2	Turn-Off Transient .....	440
6.16.3	Switching Power Losses .....	443
6.16.4	$[dV/dt]$ Capability .....	443
6.17	Safe Operating Area .....	447
6.17.1	Bipolar Second Breakdown .....	449
6.17.2	MOS Second Breakdown .....	451
6.18	Integral Body Diode .....	452
6.18.1	Reverse Recovery Enhancement .....	453
6.18.2	Impact of Parasitic Bipolar Transistor .....	453
6.19	High-Temperature Characteristics .....	454
6.19.1	Threshold Voltage .....	454
6.19.2	On-Resistance .....	455
6.19.3	Saturation Transconductance .....	456
6.20	Complementary Devices .....	457
6.20.1	The p-Channel Structure .....	458
6.20.2	On-Resistance .....	458
6.20.3	Deep-Trench Structure .....	459
6.21	Silicon Power MOSFET Process Technology .....	460
6.21.1	Planar VD-MOSFET Process .....	460
6.21.2	Trench U-MOSFET Process .....	462
6.22	Silicon Carbide Devices .....	465
6.22.1	The Baliga-Pair Configuration .....	465
6.22.2	Planar Power MOSFET Structure .....	476
6.22.3	Shielded Planar Power MOSFET Structures .....	481
6.22.4	Shielded Trench-Gate Power MOSFET Structure .....	489
6.23	Summary .....	498
	Problems .....	499
	References .....	503
<b>Chapter 7</b>	<b>Bipolar Junction Transistors .....</b>	<b>507</b>
7.1	Power Bipolar Junction Transistor Structure .....	508
7.2	Basic Operating Principles .....	510
7.3	Static Blocking Characteristics .....	513

7.3.1	Open-Emitter Breakdown Voltage .....	514
7.3.2	Open-Base Breakdown Voltage .....	514
7.3.3	Shorted Base–Emitter Operation .....	516
7.4	Current Gain .....	520
7.4.1	Emitter Injection Efficiency .....	522
7.4.2	Emitter Injection Efficiency with Recombination in the Depletion Region .....	526
7.4.3	Emitter Injection Efficiency with High-Level Injection in the Base .....	528
7.4.4	Base Transport Factor .....	533
7.4.5	Base Widening at High Collector Current Density .....	536
7.5	Emitter Current Crowding .....	550
7.5.1	Low-Level Injection in the Base .....	551
7.5.2	High-Level Injection in the Base .....	555
7.5.3	Emitter Geometry .....	559
7.6	Output Characteristics .....	560
7.7	On-State Characteristics .....	565
7.7.1	Saturation Region .....	566
7.7.2	Quasisaturation Region .....	571
7.8	Switching Characteristics .....	574
7.8.1	Turn-On Transition .....	575
7.8.2	Turn-Off Transition .....	588
7.9	Safe Operating Area .....	607
7.9.1	Forward-Biased Second Breakdown .....	608
7.9.2	Reverse-Biased Second Breakdown .....	611
7.9.3	Boundary for Safe Operating Area .....	615
7.10	Darlington Configuration .....	616
7.11	Summary .....	619
	Problems .....	619
	References .....	621
<b>Chapter 8</b>	<b>Thyristors .....</b>	<b>625</b>
8.1	Power Thyristor Structure and Operation .....	628
8.2	Blocking Characteristics .....	631
8.2.1	Reverse-Blocking Capability .....	632
8.2.2	Forward-Blocking Capability .....	636
8.2.3	Cathode Shorting .....	641
8.2.4	Cathode Shorting Geometry .....	644
8.3	On-State Characteristics .....	651
8.3.1	On-State Operation .....	652
8.3.2	Gate-Triggering Current .....	654
8.3.3	Holding Current .....	657
8.4	Switching Characteristics .....	662
8.4.1	Turn-On Time .....	663

8.4.2	Gate Design.....	671
8.4.3	Amplifying Gate Design.....	672
8.4.4	$[dV/dt]$ Capability .....	675
8.4.5	Turn-Off Process .....	683
8.5	Light-Activated Thyristors.....	685
8.5.1	$[dI/dt]$ Capability .....	686
8.5.2	Gate Region Design.....	687
8.5.3	Optically Generated Current Density .....	688
8.5.4	Amplifying Gate Design.....	690
8.6	Self-Protected Thyristors .....	691
8.6.1	Forward Breakdown Protection.....	691
8.6.2	$[dV/dt]$ Turn-On Protection .....	694
8.7	The Gate Turn-Off Thyristor Structure.....	698
8.7.1	Basic Structure and Operation.....	698
8.7.2	One-Dimensional Turn-Off Criterion.....	701
8.7.3	One-Dimensional Storage Time Analysis .....	703
8.7.4	Two-Dimensional Storage Time Model.....	704
8.7.5	One-Dimensional Voltage Rise Time Model.....	706
8.7.6	One-Dimensional Current Fall Time Model .....	709
8.7.7	Switching Energy Loss .....	721
8.7.8	Maximum Turn-Off Current.....	722
8.7.9	Cell Design and Layout .....	725
8.8	The Triac Structure.....	726
8.8.1	Basic Structure and Operation.....	728
8.8.2	Gate-Triggering Mode 1 .....	729
8.8.3	Gate-Triggering Mode 2 .....	730
8.8.4	$[dV/dt]$ Capability .....	731
8.9	Summary .....	733
	Problems.....	733
	References .....	735
<b>Chapter 9 Insulated Gate Bipolar Transistors .....</b>		<b>737</b>
9.1	Basic Device Structures .....	741
9.2	Device Operation and Output Characteristics.....	745
9.3	Device Equivalent Circuit.....	748
9.4	Blocking Characteristics .....	748
9.4.1	Symmetric Structure Forward-Blocking Capability.....	748
9.4.2	Symmetric Structure Reverse-Blocking Capability .....	753
9.4.3	Symmetric Structure Leakage Current .....	754
9.4.4	Asymmetric Structure Forward-Blocking Capability .....	760
9.4.5	Asymmetric Structure Reverse-Blocking Capability .....	767
9.4.6	Asymmetric Structure Leakage Current.....	769
9.5	On-State Characteristics.....	776
9.5.1	On-State Model.....	776

9.5.2	On-State Carrier Distribution: Symmetric Structure.....	783
9.5.3	On-State Voltage Drop: Symmetric Structure.....	791
9.5.4	On-State Carrier Distribution: Asymmetric Structure.....	796
9.5.5	On-State Voltage Drop: Asymmetric Structure .....	803
9.5.6	On-State Carrier Distribution: Transparent Emitter Structure .....	808
9.5.7	On-State Voltage Drop: Transparent Emitter Structure .....	813
9.6	Current Saturation Model.....	815
9.6.1	Carrier Distribution: Symmetric Structure .....	820
9.6.2	Output Characteristics: Symmetric Structure.....	828
9.6.3	Output Resistance: Symmetric Structure.....	833
9.6.4	Carrier Distribution: Asymmetric Structure.....	834
9.6.5	Output Characteristics: Asymmetric Structure.....	844
9.6.6	Output Resistance: Asymmetric Structure .....	848
9.6.7	Carrier Distribution: Transparent Emitter Structure .....	849
9.6.8	Output Characteristics: Transparent Emitter Structure .....	853
9.6.9	Output Resistance: Transparent Emitter Structure .....	855
9.7	Switching Characteristics.....	856
9.7.1	Turn-On Physics: Forward Recovery .....	857
9.7.2	Turn-Off Physics: No-Load Conditions .....	865
9.7.3	Turn-Off Physics: Resistive Load .....	867
9.7.4	Turn-Off Physics: Inductive Load.....	876
9.7.5	Energy Loss per Cycle.....	904
9.8	Power Loss Optimization .....	907
9.8.1	Symmetric Structure .....	907
9.8.2	Asymmetric Structure.....	909
9.8.3	Transparent Emitter Structure .....	911
9.8.4	Comparison of Tradeoff Curves .....	912
9.9	Complementary (P-Channel) Structure.....	913
9.9.1	On-State Characteristics .....	915
9.9.2	Switching Characteristics .....	919
9.9.3	Power Loss Optimization .....	919
9.10	Latch-Up Suppression.....	920
9.10.1	Deep P <sup>+</sup> Diffusion.....	922
9.10.2	Shallow P <sup>+</sup> Layer .....	928
9.10.3	Reduced Gate Oxide Thickness.....	931
9.10.4	Bipolar Current Bypass.....	936
9.10.5	Diverter Structure .....	939
9.10.6	Cell Topology .....	943
9.10.7	Latch-Up Proof Structure .....	948
9.11	Safe Operating Area.....	951
9.11.1	Forward-Biased Safe Operating Area .....	952
9.11.2	Reverse-Biased Safe Operating Area .....	956
9.11.3	Short-Circuit Safe Operating Area .....	960

9.12	Trench-Gate Structure .....	966
9.12.1	Blocking Mode .....	967
9.12.2	On-State Carrier Distribution .....	969
9.12.3	On-State Voltage Drop .....	971
9.12.4	Switching Characteristics .....	973
9.12.5	Safe Operating Area .....	974
9.12.6	Modified Structures .....	978
9.13	Blocking Voltage Scaling .....	980
9.13.1	N-Base Design .....	981
9.13.2	Power MOSFET Baseline .....	982
9.13.3	On-State Characteristics .....	982
9.13.4	Tradeoff Curve.....	985
9.14	High Temperature Operation .....	986
9.14.1	On-State Characteristics .....	986
9.14.2	Latch-Up Characteristics .....	989
9.15	Lifetime Control Techniques .....	991
9.15.1	Electron Irradiation.....	991
9.15.2	Neutron Irradiation .....	993
9.15.3	Helium Irradiation .....	993
9.16	Cell Optimization .....	994
9.16.1	Planar-Gate Structure.....	995
9.16.2	Trench-Gate Structure .....	999
9.17	Reverse Conducting Structure.....	1006
9.18	Summary .....	1014
	Problems.....	1015
	References .....	1020
<b>Chapter 10</b>	<b>Synopsis.....</b>	<b>1027</b>
10.1	Typical H-Bridge Topology .....	1027
10.2	Power Loss Analysis .....	1029
10.3	Low DC Bus Voltage Applications .....	1032
10.4	Medium DC Bus Voltage Applications .....	1037
10.5	High DC Bus Voltage Applications.....	1041
10.6	Summary .....	1045
	Problems.....	1045
	References .....	1047
	Author's Biography .....	1049
	Index .....	1053

## Chapter 1

# Introduction

Modern society is increasingly dependent upon electrical appliances for comfort, transportation, and healthcare, motivating great advances in power generation, power distribution and power management technologies. These advancements owe their allegiance to enhancements in the performance of power devices that regulate the flow of electricity. After the displacement of vacuum tubes by solid state devices in the 1950s, the industry relied upon silicon bipolar devices, such as bipolar power transistors and thyristors. Although the ratings of these devices grew rapidly to serve an ever broader system need, their fundamental limitations in terms of the cumbersome control and protection circuitry led to bulky and costly solutions. The advent of MOS technology for digital electronics enabled the creation of a new class of devices in the 1970s for power switching applications as well. These silicon power MOSFETs have found extensive use in high frequency applications with relatively low operating voltages (below 100 V). The merger of MOS and bipolar physics enabled the creation of yet another class of devices in the 1980s. The most successful innovation in this class of devices has been the insulated gate bipolar transistor (IGBT). The high power density, simple interface, and ruggedness of the IGBT have made it the technology of choice for all medium and high power applications, with perhaps the exception of high voltage DC transmission systems. Even the last remaining bastion for the conventional power thyristors is threatened by the incorporation of MOS-gated structures.

Power devices are required for systems that operate over a broad spectrum of power levels and frequencies. In Fig. 1.1, the applications for power devices are shown as a function of operating frequency. High power systems, such as HVDC power distribution and locomotive drives, requiring the control of megawatts of power operate at relatively low frequencies. As the operating frequency increases, the power ratings decrease for the devices, with typical microwave devices handling about 100 W. All these applications are served by silicon devices. Thyristors are

avored for the low frequency, high power applications, IGBTs for the medium frequency and power applications, and power MOSFETs for the high frequency applications.

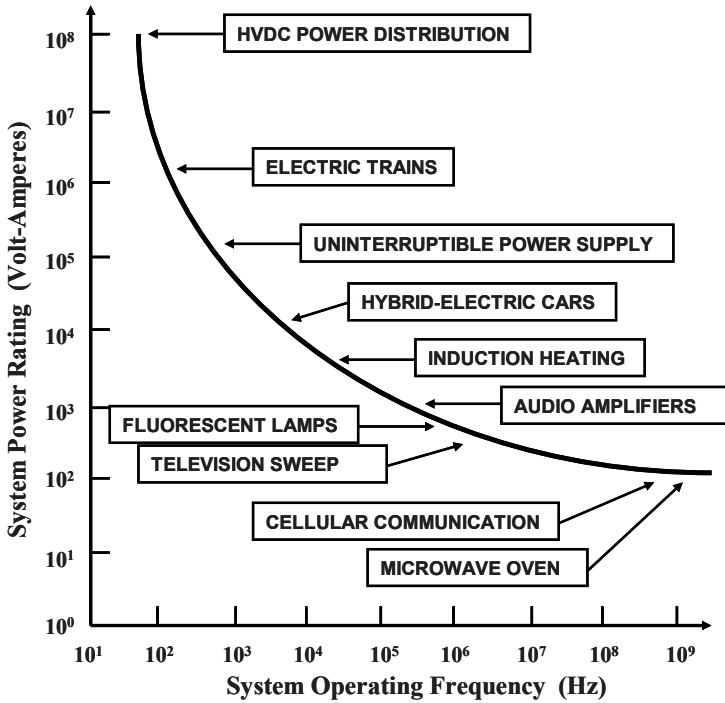


Fig. 1.1 Applications for power devices

Another approach to classification of applications for power devices is in terms of their current and voltage handling requirements, as shown in Fig. 1.2. On the high power end of the chart, thyristors are available that can individually handle over 6,000 V and 2,000 A, enabling the control of over 10 MW of power by a single monolithic device. These devices are suitable for the HVDC power transmission and locomotive drive (traction) applications. For the broad range of systems that require operating voltages between 300 and 3,000 V with significant current handling capability, the IGBT has been found to be the optimum solution. When the current requirements fall below 1 A, it is feasible to integrate multiple devices on a single monolithic chip to provide greater functionality for systems such as telecommunications and display drives. However, when the current exceeds a few amperes, it is more cost effective to use discrete power MOSFETs with appropriate control ICs to serve applications such as automotive electronics and switch mode power supplies. Consequently, no single device structure exists at this time that is suitable for serving all the applications, leaving plenty of room for further innovations.

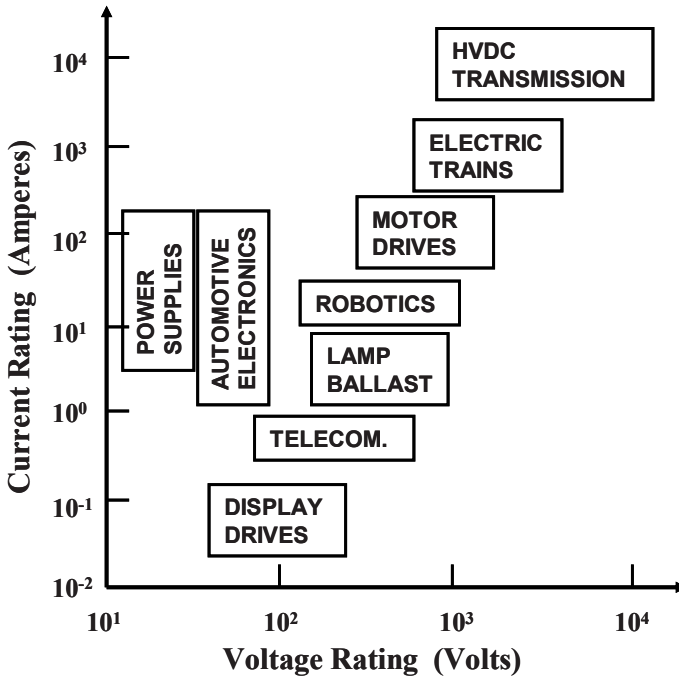


Fig. 1.2 System ratings for power devices

## 1.1 Ideal and Typical Power Switching Waveforms

An ideal power device must be capable of controlling the flow of power to loads with zero power dissipation. The loads encountered in systems may be inductive in nature (such as motors and solenoids), resistive in nature (such as heaters and lamp filaments), or capacitive in nature (such as transducers and LCD displays). Most often, the power delivered to a load is controlled by turning-on a power device on a periodic basis to generate pulses of current that can be regulated by a control circuit. The ideal waveforms for the power delivered through a power switch are shown in Fig. 1.3. During each switching cycle, the switch remains on for a time upto  $t_{ON}$  and maintains an off-state for the remainder of the period  $T$ . For an ideal power switch, the voltage drop during the on-state is zero, resulting in no power dissipation. Similarly, during the off-state, the (leakage) current in the ideal power switch is zero, resulting in no power dissipation. In addition, it is assumed that the power switch makes the transition between the on-state and off-state instantaneously, resulting in no power loss as well.

The waveforms observed with typical power switches produce power dissipation during the on-state, off-state, as well as during the switching transients. As shown in Fig. 1.4, typical power devices exhibit a voltage drop ( $V_F$ ) in the on-state, which results in a power dissipation in the on-state given by:

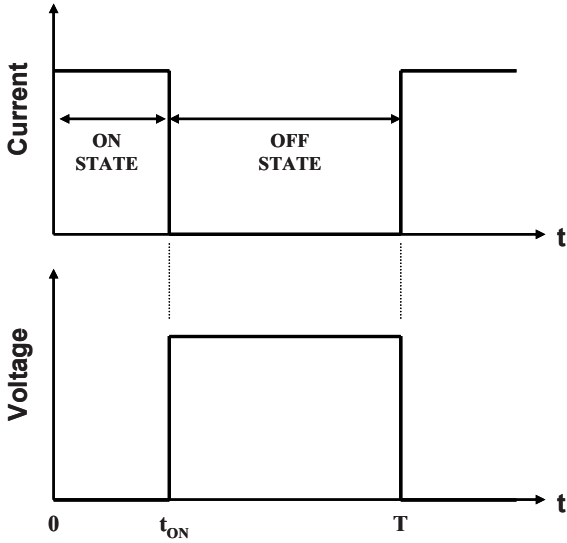


Fig. 1.3 Ideal switching waveforms for power delivery

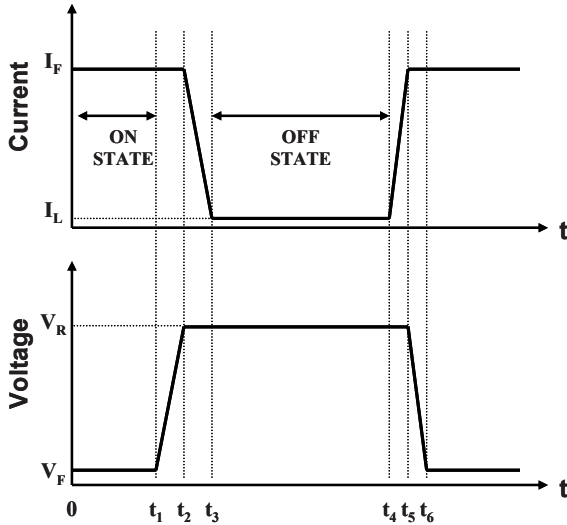


Fig. 1.4 Typical switching waveforms for power delivery

$$P_L(\text{on}) = \delta I_F V_F \tag{1.1}$$

where  $I_F$  is the on-state current. In this expression,  $\delta$  is referred to as the duty cycle given by:

$$\delta = t_1 / T \tag{1.2}$$

where  $T$  is the time period (the reciprocal of the operating frequency).

Power dissipation also occurs in the off-state given by

$$P_L(\text{off}) = (1 - \delta) I_L V_R \quad (1.3)$$

where  $I_L$  is the leakage current exhibited by the device in its off-state due to supporting a reverse bias ( $V_R$ ). This expression holds true if the switching times are small compared with the time period. If this assumption is not valid, the power dissipation can be obtained by using:

$$P_L(\text{off}) = (t_4 - t_3) I_L V_R / T \quad (1.4)$$

Most often, the power dissipation in the off-state is small when compared with the other components and can be neglected. However, this does not hold true at elevated temperatures and when Schottky contacts are supporting the reverse voltage.

The power dissipation that occurs during switching must be treated separately for the turn-off transient and the turn-on transient. During the turn-off transient for typical loads that are inductive in nature, the voltage across the switch increases rapidly to the DC-supply voltage, followed by a decrease in the current flowing through the switch. For the linearized waveforms shown in Fig. 1.4, the power loss during the turn-off transient can be calculated using:

$$P_L(\text{turnoff}) = 0.5(t_3 - t_1) I_F V_R f \quad (1.5)$$

where  $f$  is the operating frequency. In a similar manner, the power loss during the turn-on transient can be calculated using:

$$P_L(\text{turnon}) = 0.5(t_6 - t_4) I_F V_R f \quad (1.6)$$

The total power dissipation incurred in the switch is obtained by combining these terms:

$$P_L(\text{total}) = P_L(\text{on}) + P_L(\text{off}) + P_L(\text{turnoff}) + P_L(\text{turnon}) \quad (1.7)$$

At low operating frequencies, the on-state power loss is usually dominant, making it desirable to develop power switches with low on-state voltage drops. At high operating frequencies, the switching power losses are usually dominant, making it desirable to develop power switches with fast switching speeds or small transition times. Unfortunately, it is usually necessary to perform a trade off between minimizing the on-state and switching power losses in most designs. As power switch technology advances, the total power loss for the optimized design continues to reduce, providing enhancements to the efficiency of power systems.

## 1.2 Ideal and Typical Power Device Characteristics

As discussed in the previous section, silicon power devices have served the industry for well over five decades but cannot be considered to have ideal device

characteristics. In general, power electronic circuits require both rectifiers to control the direction of current flow and power switches to regulate the duration of current flow. Neither of these components exhibits the ideal characteristics that are required in power circuits to prevent power dissipation.

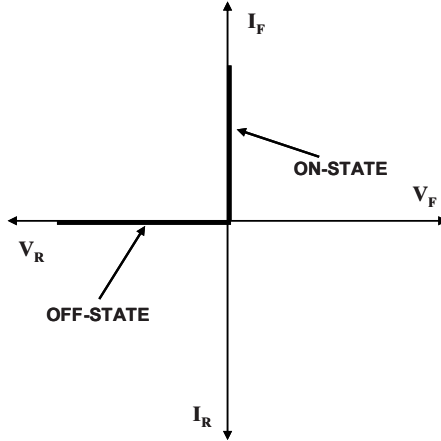


Fig. 1.5 Characteristics of an ideal power rectifier

An ideal power rectifier should exhibit the current–voltage ( $i-v$ ) characteristics shown in Fig. 1.5. In the forward conduction mode, the first quadrant of operation in the figure, it should be able to carry any amount of current with zero on-state voltage drop. In the reverse blocking mode, the third quadrant of operation in the figure, it should be able to hold off any value of voltage with zero leakage current. Further, the ideal rectifier should be able to switch between the on-state and the off-state, with zero switching time.

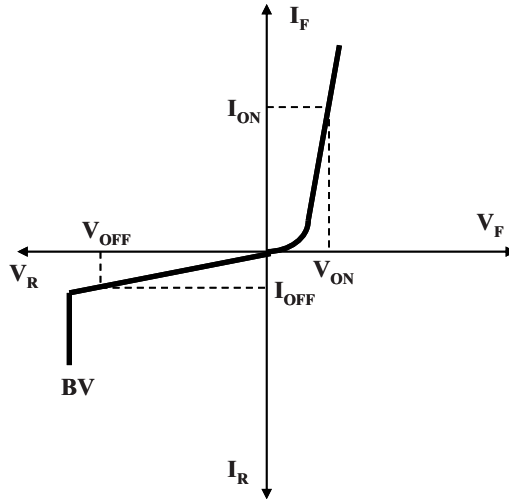


Fig. 1.6 Characteristics of a typical power rectifier

Actual silicon power rectifiers exhibit the  $i-v$  characteristics illustrated in Fig. 1.6. They have a finite voltage drop ( $V_{ON}$ ) when carrying current on the on-state, leading to “conduction” power loss. They also have a finite leakage current ( $I_{OFF}$ ) when blocking voltage in the off-state, creating off-state power loss. In addition, the doping concentration and thickness of the drift region of the silicon device must be carefully chosen with a design target for the breakdown voltage (BV). Moreover, the power dissipation in power devices increases when their voltage rating is increased because of an increase in the on-state voltage drop.

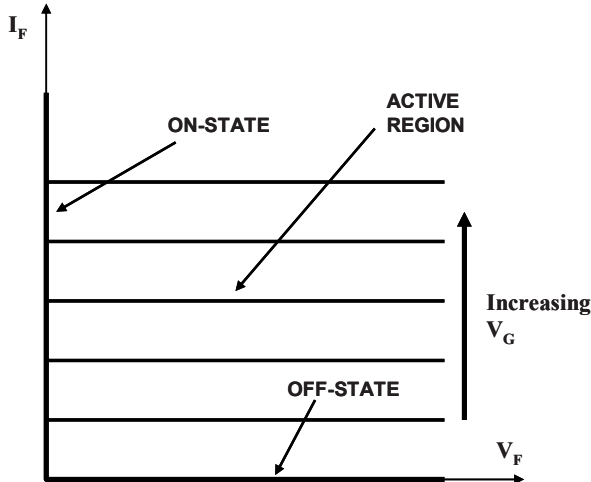


Fig. 1.7 Characteristics of an ideal transistor

The  $i-v$  characteristics of an ideal power switch are illustrated in Fig. 1.7. As in the case of the ideal rectifier, the ideal transistor conducts current in the on-state with zero voltage drop and blocks voltage in the off-state with zero leakage current. In addition, the ideal device can operate with a high current and voltage in the active region, with the saturated forward current in this mode controlled by the applied gate bias. The spacing between the characteristics in the active region is uniform for an ideal transistor indicating a gain that is independent of the forward current and voltage.

The  $i-v$  characteristics of a typical power switch are illustrated in Fig. 1.8. This device exhibits a finite resistance when carrying current in the on-state as well as a finite leakage current while operating in the off-state (not shown in the figure because its value is much lower than the on-state current levels). The breakdown voltage of a typical transistor is also finite as indicated in the figure with “BV”. The typical transistor can operate with a high current and voltage in the active region. This current is controlled by the base current for a bipolar transistor while it is determined by a gate voltage for a MOSFET or IGBT (as indicated in the figure). It is preferable to have gate voltage controlled characteristics because the drive circuit can be integrated to reduce its cost. The spacing between the

characteristics in the active region is nonuniform for a typical transistor with a square-law behavior for devices operating with channel pinch-off in the current saturation mode. Recently, devices operating under a new super-linear mode have been proposed and demonstrated for wireless base-station applications.<sup>1</sup> These devices exhibit an equal spacing between the saturated drain current characteristics as the gate voltage is increased. This is an ideal behavior when the transistor is used for the amplification of audio, video, or cellular signals because it eliminates signal distortion that occurs with the characteristics shown in Fig. 1.8.

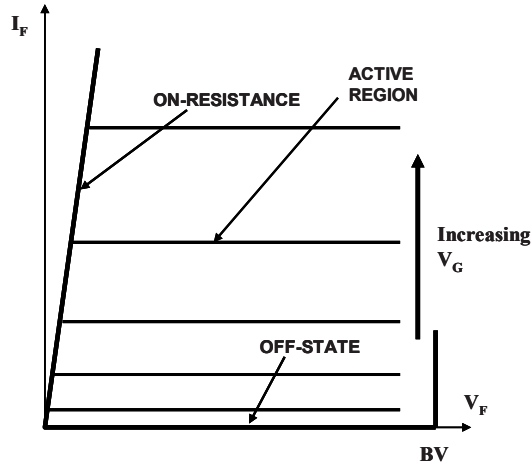


Fig. 1.8 Characteristics of a typical transistor

### 1.3 Unipolar Power Devices

Bipolar power devices operate with the injection of minority carriers during on-state current flow. These carriers must be removed when switching the device from the on-state to the off-state. This is accomplished by either charge removal via the gate drive current or via the electron-hole recombination process. These processes introduce significant power losses that degrade the power management efficiency. It is therefore preferable to utilize unipolar current conduction in a power device. The commonly used unipolar power diode structure is the Schottky rectifier that utilizes a metal-semiconductor barrier to produce current rectification. The high voltage Schottky rectifier structure also contains a drift region, as shown in Fig. 1.9, which is designed to support the reverse blocking voltage. The resistance of the drift region increases rapidly with increasing blocking voltage capability, as discussed later in this chapter. Silicon Schottky rectifiers are commercially available with blocking voltages of up to 100 V. Beyond this value, the on-state voltage drop of silicon Schottky rectifiers becomes too large for practical applications. Silicon P-i-N rectifiers are favored for designs with larger BVs due to their low on-state

voltage drop despite slower switching properties. Silicon carbide Schottky rectifiers have much lower drift region resistance, enabling design of very high voltage devices with low on-state voltage drop and excellent switching characteristics.

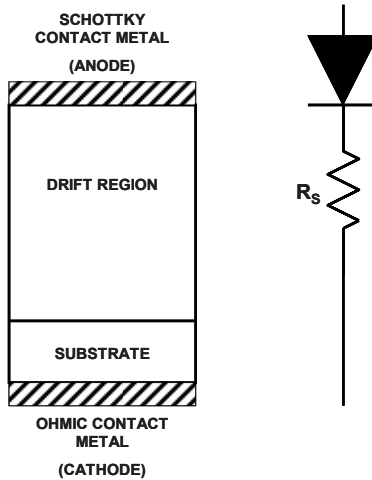


Fig. 1.9 The power Schottky rectifier structure and its equivalent circuit

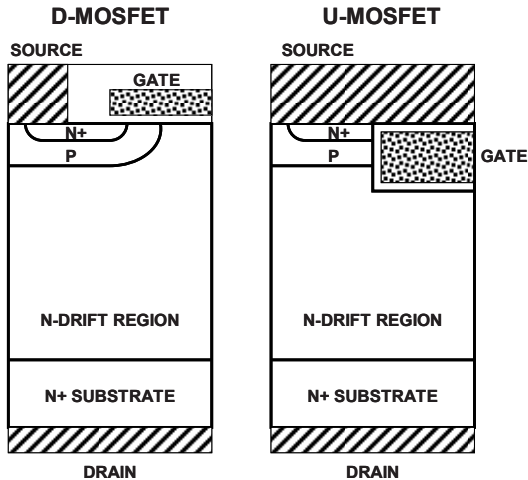


Fig. 1.10 Silicon power MOSFET structures

The most commonly used unipolar power transistor is the silicon power metal-oxide-semiconductor field-effect-transistor or MOSFET. Although other structures such as JFETs or SITs have been explored,<sup>2</sup> they have not been popular for power electronic applications because of their normally-on behavior. The commercially available silicon power MOSFETs are based upon the structures shown in Fig. 1.10. The D-MOSFET was first commercially introduced in the